## PAPER

CrossMark
click for updates

# $^{31}$P NMR characterisation of phosphate fragments during dissolution of calcium sodium phosphate glasses

Franziska Döhler,[a] Armando Mandlule,[a] Leo van Wüllen,[b] Manfred Friedrich[c] and Delia S. Brauer*[a]

Phosphate glasses in the system $P_2O_5$–$CaO$–$Na_2O$ dissolve in aqueous solutions, and their solubility can be varied by changing the glass composition. This makes them of interest for use as controlled release materials, *e.g.* as degradable implants, devices for the release of trace elements or as fertilizers, but in order to tailor glass solubility to meet specific requirements, we need to further our understanding of their dissolution behaviour and mechanism. The structure of $P_2O_5$–$CaO$–$Na_2O$ glasses ($P_2O_5$ between 55 and 35 mol%; glass structure analysed by $^{31}$P MAS NMR) changed from a network (55 mol% $P_2O_5$) to short chains (35 mol%) with decreasing phosphate content. Solubility in Tris buffer showed significant differences with phosphate content and glass structure; dissolution varied between 90% (50 mol% $P_2O_5$) and 15% (35 mol%) at 24 h. Glasses with high phosphate contents significantly lowered the pH of the solution, while glasses with low phosphate contents did not. Glasses consisting of a phosphate network dissolved by a mechanism involving P–O–P bond hydrolysis, as no $Q^3$ groups but increasing concentrations of $Q^0$ (orthophosphate) were found in solution by solution $^{31}$P NMR. Glasses consisting of chains, by contrast, can dissolve by hydration of entire chains, but hydrolysis also occurred, resulting in formation of $Q^0$ and small ring structures. This occurrence of hydrolysis (and thus formation of P–OH groups, which can be deprotonated) caused the pH decrease and explains the variation in solution pH with structure.

## 1 Introduction

Phosphate glasses are of interest for a wide range of applications, including laser glasses,[1,2] for radioactive waste entrapment,[3,4] as fertilisers in agriculture,[5] release devices for the delivery of therapeutic ions[6-8] or resorbable temporary implant materials.[9] Phosphate glasses can be water-soluble; however, the requirements for solubility vary widely with their intended use. For laser or waste entrapment applications, non-soluble glasses are needed, while for the remaining ones, some solubility is desired. In all these applications, therefore, controlling the rate of glass degradation and dissolution is key for their success.

Glass solubility depends on the phosphate content as well as the type and content of modifier cations. The solubility behaviour of sodium calcium metaphosphate glasses has been characterised by Bunker *et al.*[10] who showed that metaphosphate glasses dissolve congruently after hydration of entire phosphate chains, and that the solubility can be altered over several orders of magnitude by changing the CaO : Na$_2$O ratio. In addition, it is generally acknowledged that glass solubility decreases when moving from the ultraphosphate to the invert composition, and that phosphate glasses can alter the pH of the dissolution medium.[11] While the influence of modifier cations on the dissolution behaviour of simple phosphate glasses has been studied numerous times,[10,12-14] studies varying the phosphate content did not keep the alkaline earth : alkali cation ratio constant,[12,15] making it difficult to correlate any changes in properties with the structure of the phosphate network. A direct comparison of phosphate glasses of varying $P_2O_5$ content, and thus varying glass structure, while maintaining a constant alkaline earth : alkali cation ratio, will help to further elucidate the structure–property relationship in these materials and allow for the successful tailoring of solubility in the future.

The aim of this study was therefore to characterise the relationship between glass structure and dissolution behaviour of simple phosphate glasses in the system $P_2O_5$–$CaO$–$Na_2O$ (phosphate content between 35 and 55 mol%; constant CaO : Na$_2$O ratio), in order to understand the influence of

*a Otto Schott Institute of Materials Research, Friedrich Schiller University Jena, Fraunhoferstr. 6, 07743 Jena, Germany. E-mail: delia.brauer@uni-jena.de; Fax: +49 3641 948502; Tel: +49 3641 948510*

*b Chemical Physics and Materials Science, Institute of Physics, Augsburg University, Universitätsstr. 1, 86159 Augsburg, Germany*

*c Institute of Inorganic and Analytical Chemistry, Friedrich Schiller University Jena, Humboldtstr. 8, 07743 Jena, Germany*

This journal is © The Royal Society of Chemistry 2015

*J. Mater. Chem. B*, 2015, **3**, 1125–1134 | 1125

phosphate content on solubility, pH and dissolution mechanism.

## 2  Materials and methods

### 2.1  Glass synthesis

Glasses $xP_2O_5$—$(100 - x)/2CaO$—$(100 - x)/2$ $Na_2O$ ($x = 35$–$55$ mol%; with the CaO : $Na_2O$ ratio being kept constant) were produced by a melt-quench route. Nominal glass compositions are given in Table 1. Mixtures of $NaPO_3$, $CaPO_3$, $P_2O_5$ and $CaCO_3$ were melted for 30 min in a platinum crucible at 1200 °C in an electric furnace and quenched between brass plates.

Glass composition was analysed by dissolving the glasses in nitric acid followed by quantitative analysis using inductively coupled plasma optical emission spectroscopy (ICP-OES) as described previously.[16] Glass structure was analysed using solid-state ^{31}P magic angle spinning nuclear magnetic resonance (MAS NMR) spectroscopy experiments as shown previously.[16]

### 2.2  Dissolution studies

0.025 mol $L^{-1}$ tris(hydroxymethyl)amino methane (Tris) solution was prepared by dissolving 3.104 g of Tris in 800 mL of $dH_2O$ and adding 9 mL of 1 mol $L^{-1}$ HCl solution. The solution was heated to 37 °C, the pH adjusted to 7.40 using 1 mol $L^{-1}$ HCl solution and the volume filled to 1000 mL. 50 mg glass (125 to 315 μm particle size range) was immersed in 50 mL Tris solution for 1, 3, 5 and 7 days at 37 °C. Before and after each time period, the pH was measured (pH meter HI 8314 with pH electrode HI 1217 D, HANNA Instruments, Kehl am Rhein, Germany), samples were filtered through medium porosity filter paper (5 μm particle retention, VWR International) and acidified using nitric acid (69%). Concentrations of P, Ca and Na were analysed using ICP-OES (Varian Liberty 150, Agilent Technologies, Böblingen, Germany). Experiments were performed in duplicates, and results are presented as mean ± standard deviation (SD).

The retained powders were rinsed with acetone, dried and characterised by ICP-OES (as described previously for untreated glass powders[16]), X-ray powder diffraction (XRD; AXS-Bruker D8-Discover, CuKα, data collected at room temperature) and ^{31}P MAS NMR spectroscopy (see below).

### 2.3  Solid state ^{31}P MAS NMR spectroscopy

[31]P magic angle spinning nuclear magnetic resonance (MAS NMR) spectroscopy experiments were performed on a Bruker Avance III NMR spectrometer operating at 7.04 T with a resonance frequency of 121.5 MHz. The spectra were acquired using a 4 mm Bruker MAS probe at spinning speeds of 10 kHz and referenced against 85% $H_3PO_4$. For the glass we used a repetition time of 2000 s,[16] whereas for the experiment on the retained powder a repetition time of 60 s was used, according to the determined spin-lattice relaxation time, $T_1$, of 12 s. For deconvolution of the MAS NMR spectra, the software DMFIT[17] was used.

### 2.4  Solution ^{31}P NMR spectroscopy

For solution ^{31}P NMR experiments, 250 mg each of glasses CNP50 and CNP45 were immersed in 50 mL 0.025 mol $L^{-1}$ Tris buffer solution and kept at 37 °C for time periods between 1 and 24 hours as well as for several weeks. Experiments were performed in triplicates. At each time point, the pH was measured and a 1 mL aliquot was removed for ^{31}P NMR analysis.

Proton-coupled ^{31}P NMR measurements were performed on a Bruker Avance III 600 MHz spectrometer operating at 14.1 T. For measurements, $D_2O$ was added to the sample solution (20% of total volume). Total time of measurement duration is given in Table 2. Relative amounts of different $Q^n$ groups were obtained from the peak areas; the experimental error was about 10%. In addition, [31]P–[31]P total correlation spectroscopy (TOCSY) experiments were performed on a solution of CNP50 at 24 h.

## 3  Results

### 3.1  Glass formation and structure

Glasses were obtained in an amorphous state as shown earlier, with the analysed composition not differing significantly from the nominal one.[16] Previously, solid-state ^{31}P MAS NMR results had shown increasing network polymerisation with increasing phosphate content, from short chains (CNP35) to a phosphate network (CNP55).[16,31] P MAS NMR results on CNP50 showed that glass CNP50 consisted actually of slightly cross-linked chains (with 2% $Q^1$ ($-6.8$ ppm), 87% $Q^2$ ($-23.5$ ppm) and 11% $Q^3$ ($-29.5$ ppm), as observed for comparable metaphosphate glasses[18]) corresponding to a network connectivity of 2.09 and a cross-link density of 0.09 rather than $Q^2$ structure consisting of chains or rings only (Fig. 1). As suggested previously,[16] a non-homogeneous distribution of $Na^+$ and $Ca^{2+}$ ions in the glass (resulting in the formation of some calcium phosphate regions) may also explain the observed high-field shoulder in the ^{31}P MAS NMR spectrum.

### 3.2  pH in Tris buffer

pH of the Tris buffer solution changed after immersion of glass powders (Fig. 2a). pH decreased linearly with immersion time ($R^2$ was 0.943, 0.989 and 0.987, respectively) for glasses CNP45, CNP50 and CNP55, whereas pH of glass CNP40 first stayed relatively constant before decreasing at day 7 and pH of glass CNP35 increased initially and then also decreased at day 7.

The pH of the Tris buffer varied with phosphate content of the immersed glass, with higher $P_2O_5$ contents resulting in lower pH values (Fig. 2b; $R^2$ (day 1 to day 7) were 0.888, 0.986, 0.992 and 0.960, respectively).

Table 1  Nominal glass composition (mol%)

| Glass | $P_2O_5$ | CaO | $Na_2O$ |
|---|---|---|---|
| CNP55 | 55.0 | 22.5 | 22.5 |
| CNP50 | 50.0 | 25.0 | 25.0 |
| CNP45 | 45.0 | 27.5 | 27.5 |
| CNP40 | 40.0 | 30.0 | 30.0 |
| CNP35 | 35.0 | 32.5 | 32.5 |

1126 | J. Mater. Chem. B, 2015, 3, 1125–1134

This journal is © The Royal Society of Chemistry 2015

**Table 2**  pH (error $\pm$ 0.02; initial pH was 7.40) after immersion (250 mg glass in 50 mL Tris at 37 °C) for various time periods ($t_{im}$), and relative amounts of $Q^n$ units present in solution as determined by $^{31}P$ NMR experiments (presented as relative amounts per phosphate chain, *i.e.* per two $Q^1$ units) and calculated average chain length in solution, $L_{sol}$ ($t_{meas}$ represents the duration of the NMR measurements)

| Glass | $t_{im}$ (h) | pH | $t_{meas}$ (h) | $Q^0$ | $Q^1$ | $Q^2$ | $L_{sol}$ |
|---|---|---|---|---|---|---|---|
| CNP50 | 24 | 7.21 | 1.6 | 0.21 $\pm$ 0.02 | 2 $\pm$ 0.2 | 18.2 $\pm$ 1.8 | 20.2 $\pm$ 2.0 |
|  | 12 | 7.36 | 0.7 | 0.26 $\pm$ 0.03 | 2 $\pm$ 0.2 | 17.9 $\pm$ 1.8 | 19.9 $\pm$ 1.9 |
|  | 6 | 7.39 | 0.7 | 0.20 $\pm$ 0.02 | 2 $\pm$ 0.2 | 12.9 $\pm$ 1.3 | 14.9 $\pm$ 1.5 |
|  | 3 | 7.40 | 0.7 | 0.09 $\pm$ 0.01 | 2 $\pm$ 0.2 | 8.4 $\pm$ 0.8 | 10.4 $\pm$ 1.4 |
|  | 1 | 7.39 | 0.7 | [b] | 2 $\pm$ 0.2 | 7.0 $\pm$ 0.7 | 9.0 $\pm$ 0.9 |
| CNP45 | 24 | [a] | 2.7 | 0.09 $\pm$ 0.01 | 2 $\pm$ 0.2 | 5.8 $\pm$ 0.6 | 7.8 $\pm$ 0.8 |
|  | 5 weeks | [a] | 2.7 | 9.9 $\pm$ 0.9 | 2 $\pm$ 0.2 | 23.2 $\pm$ 2.3 | 25.2 $\pm$ 2.5 |

[a] Not measured. [b] Signal-to-noise ratio too low for reliable quantification.

### 3.3  Ion release into Tris buffer

Results of dissolution experiments are presented as absolute concentrations (in mmol L$^{-1}$; Fig. 3a–c) and as percentage relative to the amount of ions present in the glass before immersion (Fig. 3d–f). About 90% of P, Ca and Na of CNP50 were found in solution at day 1, while only between 10 and 20% of CNP35 had dissolved. The percentage of released ions increased from CNP35 to CNP50.

For glasses CNP35 to CNP50, concentrations of P, Ca and Na in Tris buffer increased dramatically during the first 24 h of immersion, reaching the maximum concentration at day 1. For glasses CNP35 and CNP40, concentrations of all three elements stayed constant throughout the remaining time of the experiment. For glasses CNP45 and CNP50, concentrations of P and Ca decreased after day three, but Na concentrations remained constant. Relative concentrations in solution (presented as a percentage of the ions present in the original glass; Fig. 4a) at early time points were comparable for P, Ca and Na, suggesting congruent dissolution, *i.e.* no selective leaching of some of the glass components. For glasses CNP35 to CNP50, the percentage of ions in solution at day 1 increased linearly with P$_2$O$_5$ content ($R^2 = 0.994$).

Glass CNP55 showed a different dissolution pattern, with concentrations of P, Ca and Na increasing continuously throughout the 7 day period. Ion release from glass CNP55 plotted *vs.* the square root of time (Fig. 4b) showed a linear increase in Ca and Na concentrations ($R^2 = 0.995$ and $0.999$, respectively), but for P the increase was linear between day 0 and 5 only ($R^2 = 0.998$). The results for all other glasses did not show a linear relationship for the time points investigated (results not shown).
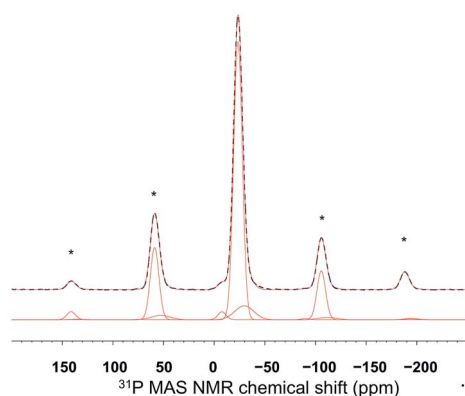


**Fig. 1** $^{31}P$ MAS NMR spectrum of glass CNP50 (dashed black curve) together with the result of a deconvolution (red curve) into three Gaussian lines (lower red curves) at −7.6 ppm (2% of total signal), −23.5 ppm (87%) and −29.7 ppm (11%). For the calculation, spinning sidebands (marked by asterisks) were taken into account.
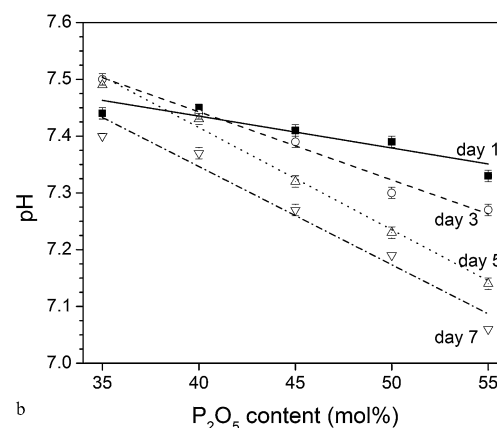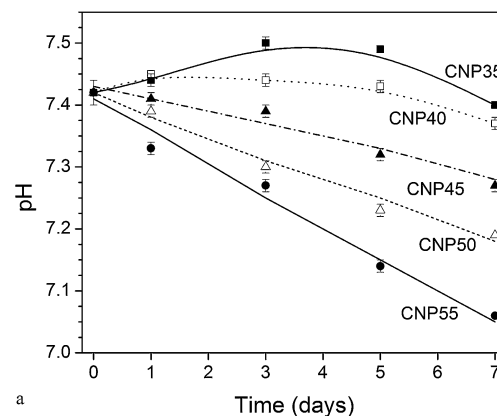


**Fig. 2** pH in Tris buffer solution: (a) pH *vs.* time and (b) pH *vs.* nominal P$_2$O$_5$ content ($\pm$SD) (straight lines are linear regression; for coefficients of determination refer to the text).
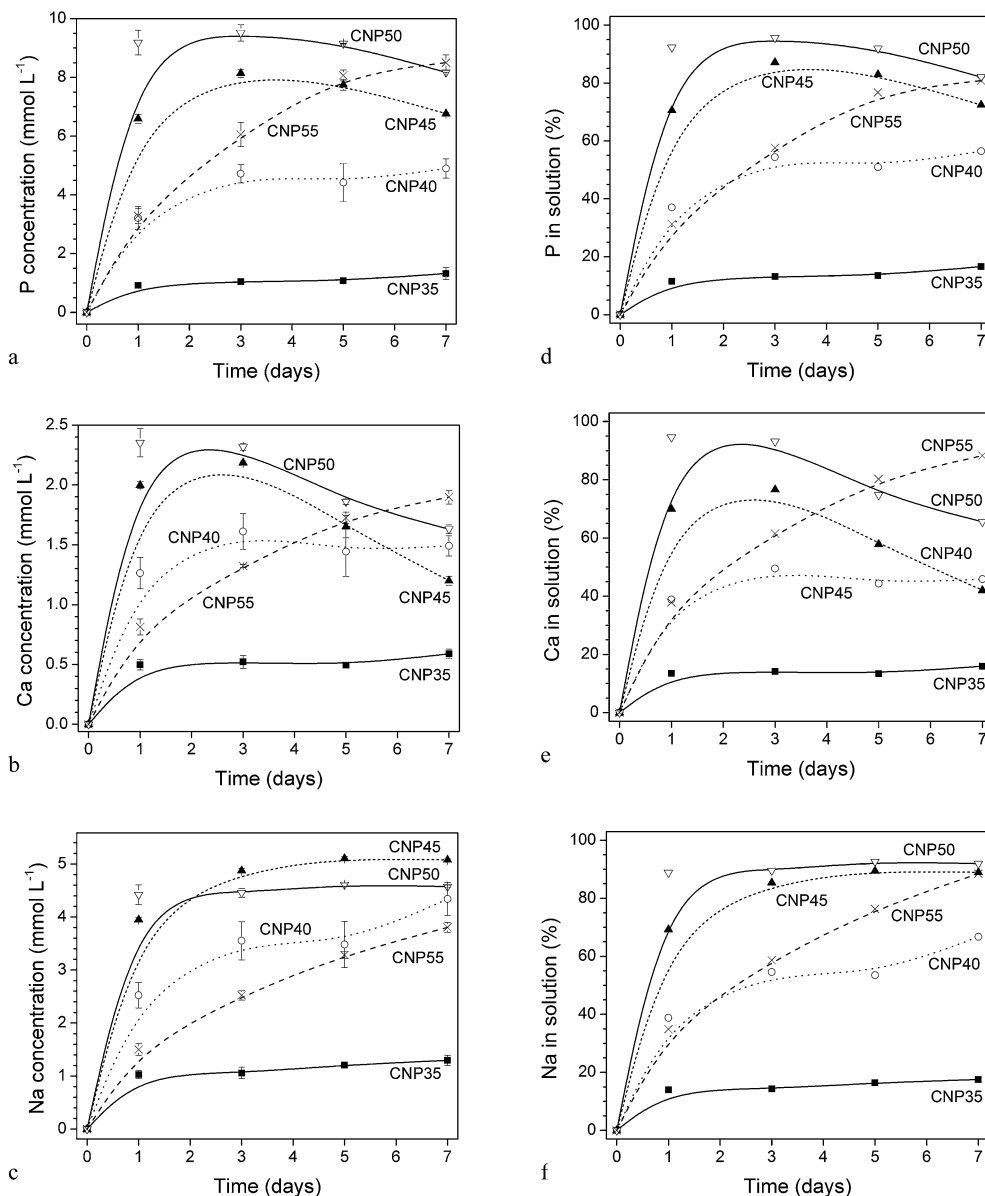
Fig. 3 Ionic concentrations in Tris buffer solution: (a–c) concentrations in mmol $L^{-1}$ (±SD) and (d–f) percentage of ions in solution *vs.* time (for error bars refer to figures a–c) (lines are visual guides only).

## 3.4 Structural units present in solution

Solution $^{31}P$ NMR experiments were performed on those glasses only, which showed fastest dissolution, CNP50 and CNP45. $^{31}P$ NMR spectra of the solutions showed multiple peaks in three areas: between about 4 to 0 ppm, −5 to −12 ppm and 18 to −25 ppm (Fig. 5a), which can be assigned to $Q^0$, $Q^1$ and $Q^2$ structural units, respectively. Relative amounts of structural units were obtained from the corresponding peak areas and are given in Table 2 (also giving the pH of the solution at each time point).

The relative amounts of $Q^0$ per phosphate chain (*i.e.* amounts of $Q^0$ per two $Q^1$ units) after dissolution of CNP45 increased from 0.09 (at 24 hours) to 9.95 (at 5 weeks; Table 2). CNP50 showed the same trend, with 0.09 (3 hours) to 0.21 (24 hours) $Q^0$ units per two $Q^1$ units. Simultaneously, the relative

amount of $Q^2$ groups per two $Q^1$ units increased from 7 (at 1 hour) to 18 (at 24 hours).

A $^{31}P$–$^{31}P$ TOCSY spectrum (Fig. 5b) of a solution of glass CNP50 at 24 h in Tris buffer showed cross-peaks corresponding to coupling between $^{31}P$ nuclei in $Q^1$ and $Q^2$ groups, showing $Q^1$ groups acting as chain end groups (rather than being present as pyrophosphate, $P_2O_7^{4-}$, only). The presence of cross-peaks in the $Q^2$ region suggests $Q^2$ groups of different chemical environments, *e.g.* $Q^2$ connected to $Q^1$ or $Q^2$ connected to $Q^2$ only.

## 3.5 Characterisation of powders after treatment in Tris buffer

Characterisation of CNP50 glass powder at 7 days in Tris using XRD showed that the amorphous halo had been replaced by
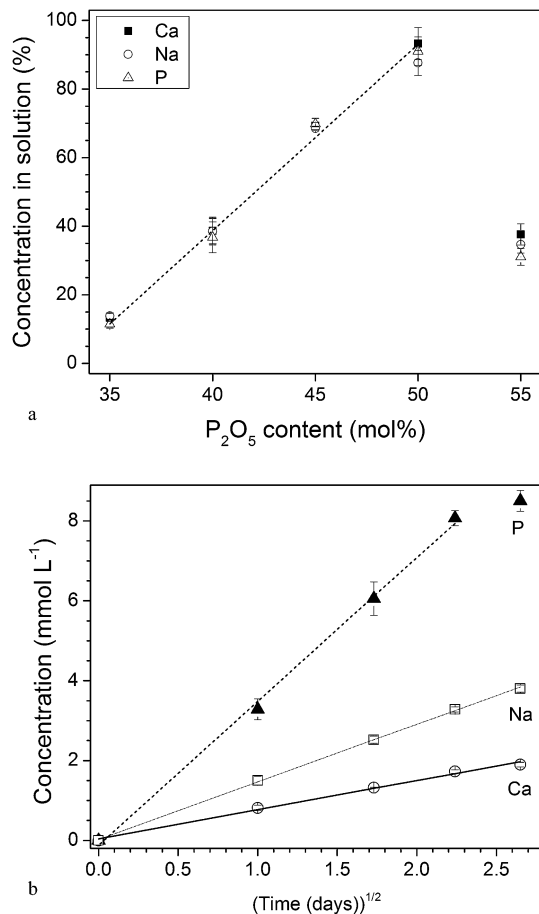
**Fig. 4** (a) Percentage of ions in solution at day 1 *vs.* $P_2O_5$ content in the glass. Line is linear regression; $R^2 = 0.994$. (b) Ions released from glass CNP55 *vs.* the square root of time. Lines are linear regression; $R^2 = 0.998$ (P), 0.995 (Ca) and 0.999 (Na), respectively.

various broad, low intensity reflections (Fig. 6a). Reflections were compared to some calcium phosphates (including $CaH_2(PO_3)_4$, JCPDS 1-86-1265; $Ca(H_2PO_4)_2 \times H_2O$, JCPDS 9-347; $Ca(H_2PO_4)_2$, JCPDS 9-390 and hydroxyapatite, $Ca_5(PO_4)_3OH$, JCPDS 9-432) of the database of the International Centre for Diffraction Data, but owing to low intensities, assigning the reflections to crystal phases was not possible. $^{31}P$ MAS NMR results showed three main signals, with cross-polarisation suggesting presence of $^1H$ (such as OH groups). The signals can be assigned to $Q^0$ (1.1 ppm; 12%), $Q^1$ (−7.6 ppm; 64%) and $Q^2$ (−21.2 ppm; 24%) of either crystalline or amorphous phases (Fig. 6b). ICP-OES analysis gave a composition (mean ± 95% confidence interval) of 37.6 (±0.1) mol% $P_2O_5$, 61.5 (±1.1) mol% CaO and 0.92 (±0.01) mol% $Na_2O$; Ca/P ratio was 0.82.

## 4   Discussion

Phosphate glasses in the system $P_2O_5$–CaO–$Na_2O$ are known to dissolve in water, and controlling their solubility is key for applications such as resorbable implants[19] or controlled release devices.[20] Varying the phosphate content has a pronounced influence on the dissolution behaviour of the glasses, caused by

changes in the glass structure. In the present study, the *glass structure* changed from a network (CNP55) to short chains (CNP35) with decreasing phosphate content.[16] All compositions with phosphate contents below 50 mol% consisted of $Q^2$ and $Q^1$ units exclusively, with the chain length decreasing with decreasing phosphate content. Glasses with 50 mol% $P_2O_5$ theoretically consist of $Q^2$ groups only, corresponding to chains of infinite length; however, glass CNP50 was shown to contain both $Q^1$ and $Q^3$ as well, thereby having a slightly cross-linked phosphate network. CNP55 also consisted of a phosphate network.[16] In the phosphate glasses characterised here, $Na^+$ and $Ca^{2+}$ modifier cations charge-balance the non-bridging oxygens (NBO) present in the structure, but will also interact with bridging oxygens (BO).[21] Depending on the Ca : Na ratio surrounding a phosphate tetrahedron (*i.e.* a $Q^n$ group), the chemical shift can be expected to vary slightly; however, $^{31}P$ MAS NMR cannot resolve these differences owing to line broadening.

Some phosphate glasses are known to affect the *pH* of the surrounding aqueous medium during dissolution, and the results here confirmed this. There was a strong influence of phosphate content and glass structure on the pH, with glasses CNP55 to CNP45 showing a pH decrease, CNP40 showing a constant pH and CNP35 showing an initial pH increase, with the pH remaining constant afterwards. (The pH decrease observed for CNP40 and CNP35 between days 5 and 7 may actually be caused by dissolution of atmospheric $CO_2$, an effect which is commonly observed during immersion studies.[22]) The pH results suggest that phosphate glasses consisting of either cross-linked chains (NC > 2) or chains above a certain length decrease the pH, while more disrupted glasses (consisting of short chains only) do not cause a pH decrease and may even cause a slight pH increase.

This slight pH rise observed for CNP35 is interesting. A pH rise typically observed upon immersion of silicate glasses or bioactive phospho-silicate glasses,[23,24] and (together with the release of calcium and phosphate ions) it favours the deposition of an apatite surface layer,[25] allowing for cell attachment[26,27] and, ultimately, bonding to bone.[28] The pH rise observed for CNP35 might suggest a dissolution behaviour somewhat similar to that of silicate glasses. However, all glasses in this study showed comparable relative concentrations (in %) of P, Ca and Na at early time points, suggesting that no selective leaching occurred, and the glasses dissolved congruently instead. This is in contrast to the dissolution behaviour observed for silicate glasses, were modifier cations are leached out from the glass, being replaced by protons from the aqueous solution, with the silicate network remaining behind as a silica gel, containing silanol groups (Si–OH).[23]

Phosphate content and glass structure greatly affected glass *solubility*; however, all glasses dissolved congruently and no selective ion leaching was observed. The dissolution pattern of glass CNP55 differed significantly from all other compositions. Release of ions from CNP55 was linear when plotted *vs.* the square root of time, suggesting diffusion controlled dissolution kinetics up to day 5 (P) and 7 (Ca, Na). For all other glasses, by contrast, diffusion controlled processes (if any) may have ended
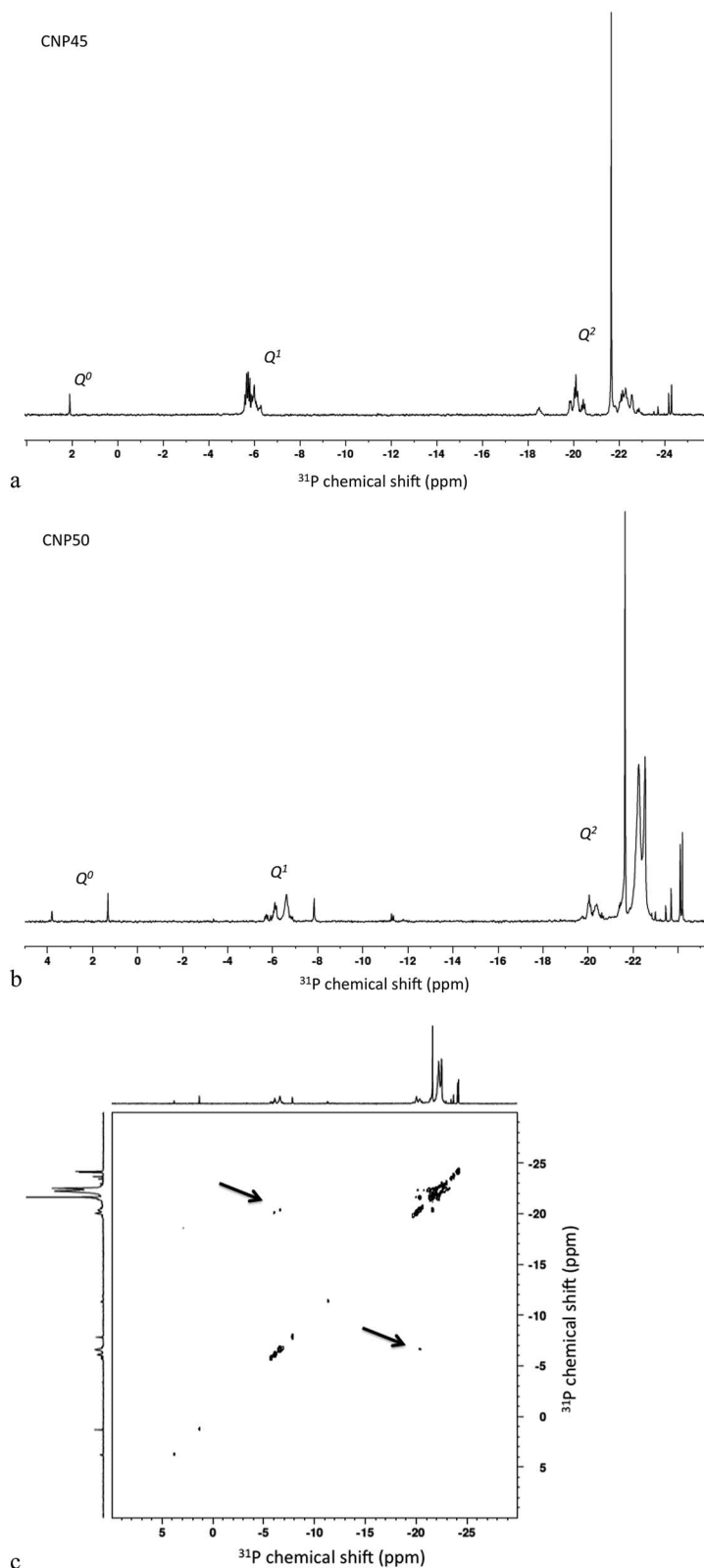
This journal is © The Royal Society of Chemistry 2015

*J. Mater. Chem. B*, 2015, **3**, 1125–1134 | **1129**

Fig. 5 $^{31}P$ NMR spectra of solutions of glasses (a) CNP45 and (b) CNP50 and (c) $^{31}P-^{31}P$ TOCSY spectrum of solution of glass CNP50 at 24 h in Tris buffer (cross-peaks corresponding to coupling between $^{31}P$ nuclei in $Q^1$ and $Q^2$ groups highlighted by arrows).

within the first 24 hours of the experiment, as no linear trend between ion release and the square root of time was observed between day 1 and 7. This shows a much slower initial dissolution rate in CNP55 compared to CNP50 and CNP45, and can be explained by the network structure of CNP55,[16] which makes hydrolysis of P–O–P bonds necessary.

1130 | J. Mater. Chem. B, 2015, 3, 1125–1134

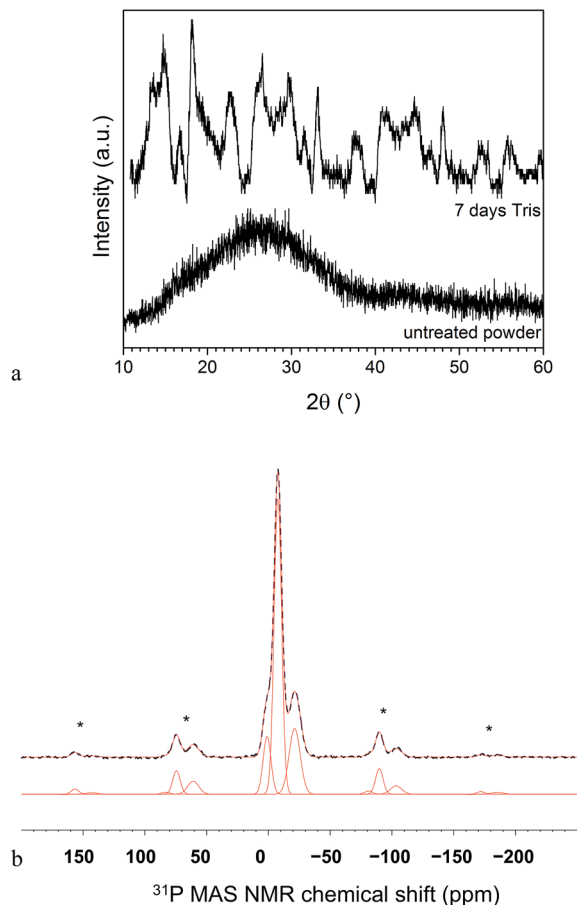This journal is © The Royal Society of Chemistry 2015

**Fig. 6** (a) XRD patterns of CNP50 glass powder before (bottom) and after (top) immersion in Tris buffer for 7 days, (b) $^{31}$P MAS NMR spectrum (dashed black curve) together with the result of a deconvolution (red curve) into three Gaussian lines (lower red curves) at +1.1 ppm (12% of total signal), −7.6 ppm (64%) and −21.2 ppm (24%). For the calculation, spinning sidebands (marked by asterisks) were taken into account.

When investigating the dissolution mechanism of phosphate glasses, two processes must be considered: dissolution by hydration of entire chains and hydrolysis of P–O–P bonds. Polyphosphate glasses consisting of phosphate chains can dissolve by hydration of entire chains,[10] and no bond hydrolysis is necessary for glass dissolution (although it may occur). By contrast, for dissolution of ultraphosphate glasses (consisting of a network structure), P–O–P linkages need to be broken. The activation energy for P–O–P hydrolysis has been shown to be significantly higher than the activation energy for glass dissolution by chain hydration.[10] Therefore, one might expect lower initial dissolution rates in glasses requiring P–O–P hydrolysis for dissolution (i.e. glasses with a network structure) compared to glasses dissolving by chain hydration (i.e. glasses with a chain structure). This can explain the lower initial dissolution rate of glass CNP55 compared to CNP50 or CNP45. Initially, P–O–P bonds had to be hydrolysed in CNP55 for dissolution to occur; however, afterwards phosphate fragments may be hydrated and go into solution, accelerating the dissolution process. At day 7, between 80 and 90% of glass CNP had dissolved.

Of all $Q$ groups present in phosphate glasses, $Q^3$ groups are the most prone to hydrolysis. van Wazer & Holst[29] explained this by delocalisation of the electrons of the double bonded oxygen in $Q^2$, $Q^1$ and $Q^0$ structural units resulting in a more stable state. In $Q^3$ structural units no resonance between different structures is possible, and this higher energetic state is more prone to hydrolysis. This means that branching $Q^3$ units are too unstable to be found in aqueous solution,[29] a finding termed the "anti-branching rule",[30] and it explains why in the present study $Q^0$, $Q^1$ and $Q^2$ were detected in solution, but no $Q^3$.

It is interesting to note that the ion release patterns of glass CNP50 were more similar to those of CNP45 than CNP55, although according to $^{31}$P MAS NMR results both CNP55 and CNP50 had network structures, while CNP45 (and all other glasses) consisted of chains.[16] The reason may be a much lower cross-link density in CNP50 (0.06) compared to CNP55 (0.20),[16] reducing the need for P–O–P bond hydrolysis owing to the presence of a larger number of chain-terminating $Q^1$ units (and therefore possible presence of chains allowing for some dissolution by chain hydration) in CNP50 but not in CNP55.

The Na release patterns of glasses CNP50 to CNP35 were very similar, while (both absolute and relative) concentrations differed significantly. CNP50 showed the fastest initial dissolution of all glasses in this study within the time investigated, with about 90% of the glass being dissolved at day 1. Solubility decreased with decreasing phosphate content, suggesting that shorter phosphate units are less easily hydrated than longer ones. And indeed the chemical durability of high iron/low phosphate content glasses for radioactive waste entrapment is very low and has been shown to be similar to that of borosilicate glass waste forms.[4]

*Solution $^{31}$P NMR* addressed three main questions: do the phosphate chains present in the glass stay intact during dissolution (as suggested by Bunker *et al.*[10])? Does hydrolysis of P–O–P bonds occur? And, if chains are present in solution, do they change (*e.g.* in length) over time?

In contrast to (solid-state) $^{31}$P MAS NMR results, where broad peaks were observed only, solution $^{31}$P NMR results showed the presence of a large number of narrow peaks. These peaks were, however, grouped, appearing in the chemical shift ranges typical for $Q^0$, $Q^1$ and $Q^2$ units. $^{31}$P NMR chemical shifts vary for different $Q^n$ structures owing to differences in their electronic environment, and $^{31}$P NMR can thus distinguish between different $Q^n$ structures. However, NMR spectra of solids show a pronounced line broadening owing to various interactions,[31] and while spinning at the magic angle can significantly reduce some of these interactions, the signals obtained from solids are much broader than those obtained from solution NMR. The actual signal position is not only dependent on the type of $Q^n$ group and (particularly in the solid glass) of the type of modifier connected to it, but it also depends on the neighbouring groups (*e.g.* $Q^1$ or $Q^2$),[32] and it is known that structural groups present in rings give a different chemical shift to the same group not present in rings.[33] While (solid-state) $^{13}$P MAS NMR cannot resolve these differences easily,[34] solution $^{31}$P NMR can, and we thus conclude that the large number of peaks observed in

solution $^{31}$P NMR originated from $Q$ units of varying $Q^n$ neighbours.

The presence of $Q^1$ and $Q^2$ units in solution indicates the presence of pyrophosphate ($Q^1$–$Q^1$), rings ($Q^2$ only) or phosphate chains ($Q^2$ middle groups with $Q^1$ end groups). TOCSY spectra showing coupling between different $Q^n$ groups, can help to elucidate which of these may exist. TOCSY spectra showed that out of the three different $Q^1$ signals, two had cross-peaks with $Q^2$ groups (i.e. the $Q^2$ signals present at about −20 ppm), suggesting that a majority of $Q^1$ groups is present in chains, but that we may have presence of pyrophosphate ($P_2O_7^{4-}$) units. The $Q^2$ peaks themselves also showed some cross-peaks to other $Q^2$ peaks, suggesting the presence of chain lengths of five or more $Q$ groups, as well as chains of various lengths.

This suggests that the glasses may indeed go into solution by hydration of chains, as presented by Bunker et al.[10] If we assume the absence of pyrophosphate ($P_2O_7^{4-}$, $Q^1$ only) and of rings ($Q^2$ only), we can estimate chain lengths based on the $Q^1 : Q^2$ ratio, and (considering two $Q^1$ units per chain), average chain lengths of 20 and 8 phosphate tetrahedra can be calculated for CNP50 and CNP45, respectively. The value obtained for CNP45 is comparable to the average chain length in the glass (9.5 phosphate tetrahedra)[16] as obtained by solid-state $^{31}$P MAS NMR. Results for solutions of CNP50, however, cannot be directly compared to the chain length in the glass, as the glass consisted of a network structure.

As orthophosphate groups ($Q^0$) were detected in all solutions investigated, the results do suggest that P–O–P hydrolysis occurred in addition to dissolution by chain hydration. The dramatic increase in the number of orthophosphate groups with time (for both CNP45 and CNP50) suggests continuing P–O–P hydrolysis over time. This can explain the drop in pH observed during immersion of phosphate glasses in Tris buffer. If glasses dissolved by hydration of entire chains only, no change in pH would be expected. However, by P–O–P hydrolysis P–OH groups are formed, which can be deprotonated, depending on $pK_a$ and solution pH,[30] resulting in a pH decrease. As P–O–P bond hydrolysis is acid catalysed, hydrolysis of phosphate chains can be expected more readily at low pH. In addition, at low pH, non-bridging oxygens (P–O$^-$ M$^+$, with M$^+$ being a modifier cation) in the glass can be protonated,[10] leading to faster water penetration into the glass and thus even faster dissolution.

Relative amounts of $Q^0$ were higher for solutions of CNP50 than CNP45, suggesting faster hydrolysis, thereby confirming the ICP-OES results and the lower pH values obtained for CNP50 compared to CNP45. As CNP50 consisted of a network rather than chains, some P–O–P bond hydrolysis had to occur during dissolution, and thus a lower pH would be expected compared to a glass which consists of chains only and thus can theoretically dissolve without hydrolysis occurring. The resistance to chain hydrolysis increases with decreasing chain length, as can be seen in the lower degradation rates of pyrophosphoric acid compared to triphosphoric acid.[35] This may explain the slower and more controlled dissolution behaviour observed for invert glasses compared to glasses in the metaphosphate

compositional range[11,36] and the decrease in solubility with decreasing phosphate content observed here.

The increasing relative concentrations of $Q^2$ groups with time seem to suggest increasing chain lengths (Table 2), which contradicts the increasing relative concentrations of $Q^0$ groups (suggesting increasing hydrolysis), particularly as it has been shown that repolymerisation of phosphates does not occur under normal conditions.[30] An alternative explanation might be that over time, rings consisting of $Q^2$ only were formed, but unfortunately, TOCSY results, while telling us that $Q^1$ groups are neighbouring some $Q^2$ groups, cannot give reliable information on the presence of rings ($Q^2$ only) or pyrophosphate structures ($Q^1$ only). However, during dissolution of Graham's salt (sodium metaphosphate glass) at high temperatures a build-up of trimetaphosphate (a ring consisting of three $Q^2$ groups; $P_3O_9^{3-}$) was observed at various pH values using paper chromatography methods,[37] while ion chromatography studies on $P_2O_5$–CaO–Na$_2$O polyphosphate glasses (45 mol% $P_2O_5$) also found trimetaphosphate rings besides pyrophosphate ($P_2O_7^{4-}$), three-membered chains ($P_3O_{10}^{5-}$) and some unidentified groups.[38]

The results presented here show that owing to P–O–P bond hydrolysis occurring simultaneously to chain hydration (although varying in rate), chain lengths found in solution are likely to be shorter than those in the glass, particularly for glasses dissolving slowly, which may be of implication for structural studies on certain phosphate glasses (particularly those of low solubility) by chromatography methods.[39]

Further experiments are necessary to fully understand the dissolution mechanism of phosphate glasses, particularly the presence of rings, when they form (if at all), and if this depends on the phosphate content in the glass. In addition, external reference standards should be used during $^{31}$P NMR experiments, in order to determine the absolute concentrations of $Q^n$ species.

For glasses CNP50 and CNP45, concentrations of Ca and P decreased from day 3 (while Na concentrations did not), suggesting precipitation of a calcium phosphate, which was confirmed by ICP-OES analysis of the powders. As apatites show the lowest solubility of all calcium phosphates in the pH range observed here,[40] precipitation of an apatite-like phase might be expected. However, based on the XRD results, the resulting phases could not be identified. The reason might be the presence of mixtures of crystalline and amorphous phases, poor crystallinity owing to substitutions in the crystal lattice, small crystallite sizes[41] or a combination of factors. $^{31}$P MAS NMR results, however, do suggest presence of mostly $Q^1$ (64%; besides 12% $Q^0$ and 24% $Q^2$), i.e. pyrophosphate species. The $Q^2$ signal (with its chemical shift of 21 ppm) suggests presence of sodium metaphosphate, which may indicate some unreacted glass phase. However, considering that at 7 days 90% of sodium had been released from the glass, the amount of unreacted sodium metaphosphate can be expected to be small, in agreement with chemical analysis of the powder. In addition, the absence of an amorphous halo in the XRD pattern confirms that no significant amounts of unreacted (amorphous) glass phase were left. $Q^2$ in calcium phosphates usually gives signals at

more negative chemical shifts ($-28$ ppm); however, Roiland *et al.*[32] have shown that in $CaO$–$P_2O_5$ glasses this position moves to more positive chemical shifts ($-20.5$ ppm for a $Q^2$ with two neighbouring $Q^1$ groups) with increasing CaO content. We can therefore conclude that $^{31}P$ MAS NMR shows presence of calcium phosphates mostly, in agreement with ICP-OES results. When assuming presence of about 38 mol% $P_2O_5$ (based on ICP-OES results), the 62 mol% CaO and $Na_2O$ detected by ICP-OES are not sufficient for forming 12% $Q^0$, 64% $Q^1$ and 24% $Q^2$ (based on $^{31}P$ MAS NMR). We would need about 71 mol% of CaO (and $Na_2O$) for charge-balancing of all NBO present (or, rather, 34.9 mol% $P_2O_5$ and 65.1 mol% CaO and $Na_2O$), which suggests presence of some OH-groups, which is in agreement with presence of $^1H$ detected by cross-polarisation during $^{31}P$ MAS NMR experiments.

Using $^{17}O$ MAS NMR, Forler *et al.*[42] have recently shown formation of orthophosphate ($NaH_2PO_4$ and $NaH_2PO_4 \times H_2O$) and pyrophosphate species ($Na_2H_2P_2O_7$) as well as amorphous phases during degradation of a sodium metaphosphate glass ($P_2O_5$–$Na_2O$), showing that the degradation mechanism is a complicated one and a range of intermediate phases can form, indicated by various proton species in $^1H$ MAS NMR.[43] These results also suggest that crystalline phases may either precipitate from the solution (as in the present study) or form on the glass surface during the alteration process.

It is interesting to note that precipitation occurred only for the glasses, which gave the lowest pH values; however, this may be explained by their high ionic concentrations in solution. Concentrations occurring during dissolution of the invert glass compositions (CNP35 and CNP40) may simply be too low for any ortho- or pyrophosphate species to precipitate.

## 5  Conclusions

Varying the phosphate content in $P_2O_5$–CaO–$Na_2O$ glasses, and thereby changing the structure from network (55 mol%) to short chains (35 mol%), dramatically altered the dissolution behaviour. Glasses with high phosphate contents significantly lowered the pH of the solution caused by a major contribution of P–O–P bond hydrolysis, while glasses with lower phosphate contents, which dissolved by a combination of chain hydration and hydrolysis, affected the pH slightly only. The dissolution mechanism changed with structure, as glasses consisting of a network structure showed a diffusion-controlled dissolution mechanism over a week, while glasses consisting of chains did not. While all glasses consisting of chains showed comparable dissolution patterns (and all dissolved congruently), their solubility varied between 90% (50 mol% $P_2O_5$) and 15% (35 mol%) with phosphate content. Taken together, the results show that hydrolysis played a major role in glasses with network structures only, but occurred during dissolution of glasses with chain structures as well.

## Acknowledgements

## References

1 V. Petrov, U. Griebner, D. Ehrt and W. Seeber, *Opt. Lett.*, 1997, **22**, 408–410.
2 J. F. Philipps, T. Topfer, H. Ebendorff-Heidepriem, D. Ehrt, R. Sauerbrey and N. F. Borrelli, *Appl. Phys. B: Lasers Opt.*, 2001, **72**, 175–178.
3 P. A. Bingham, R. J. Hand, O. M. Hannant, S. D. Forder and S. H. Kilcoyne, *J. Non-Cryst. Solids*, 2009, **355**, 1526–1538.
4 D. E. Day, Z. Wu, C. S. Ray and P. Hrma, *J. Non-Cryst. Solids*, 1998, **241**, 1–12.
5 P. Knott, *Glastech. Ber.*, 1989, **62**, 29–34.
6 J. P. Pessan, N. S. Al-Ibrahim, M. A. R. Buzalaf and K. J. Toumba, *J. Appl. Oral Sci.*, 2008, **16**, 238–246.
7 W. M. Allen, B. F. Sansom, P. T. Gleed, C. B. Mallinson and C. F. Drake, *Vet. Rec.*, 1984, **115**, 55–57.
8 W. M. Allen, B. F. Sansom, C. B. Mallinson, R. J. Stebbings and C. F. Drake, *Vet. Rec.*, 1985, **116**, 175–177.
9 E. A. Abou Neel, D. M. Pickup, S. P. Valappil, R. J. Newport and J. C. Knowles, *J. Mater. Chem.*, 2009, **19**, 690–701.
10 B. C. Bunker, G. W. Arnold and J. A. Wilder, *J. Non-Cryst. Solids*, 1984, **64**, 291–316.
11 D. S. Brauer, C. Rüssel and J. Kraft, *J. Non-Cryst. Solids*, 2007, **353**, 263–270.
12 I. Ahmed, M. Lewis, I. Olsen and J. C. Knowles, *Biomaterials*, 2004, **25**, 491–499.
13 K. Franks, I. Abrahams, G. Georgiou and J. C. Knowles, *Biomaterials*, 2001, **22**, 497–501.
14 K. Franks, I. Abrahams and J. C. Knowles, *J. Mater. Sci.: Mater. Med.*, 2000, **11**, 609–614.
15 M. Uo, M. Mizuno, Y. Kuboki, A. Makishima and F. Watari, *Biomaterials*, 1998, **19**, 2277–2284.
16 A. Mandlule, F. Döhler, L. van Wüllen, T. Kasuga and D. S. Brauer, *J. Non-Cryst. Solids*, 2014, **392–393**, 31–38.
17 D. Massiot, F. Fayon, M. Capron, I. King, S. Le Calve, B. Alonso, J. O. Durand, B. Bujoli, Z. H. Gan and G. Hoatson, *Magn. Reson. Chem.*, 2002, **40**, 70–76.
18 E. A. Abou Neel, W. Chrzanowski, D. M. Pickup, L. A. O'Dell, N. J. Mordan, R. J. Newport, M. E. Smith and J. C. Knowles, *J. R. Soc., Interface*, 2009, **6**, 435–446.
19 M. Bitar, J. C. Knowles, M. P. Lewis and V. Salih, *J. Mater. Sci.: Mater. Med.*, 2005, **16**, 1131–1136.
20 A. G. Avent, C. N. Carpenter, J. D. Smith, D. M. Healy and T. Gilchrist, *J. Non-Cryst. Solids*, 2003, **328**, 31–39.
21 R. I. Ainsworth, D. Di Tommaso, J. K. Christie and N. H. de Leeuw, *J. Chem. Phys.*, 2012, **137**, 234502.
22 Y. C. Fredholm, N. Karpukhina, D. S. Brauer, J. R. Jones, R. V. Law and R. G. Hill, *J. R. Soc., Interface*, 2012, **9**, 880–889.
23 S. Fagerlund, L. Hupa and M. Hupa, *Acta Biomater.*, 2013, **9**, 5400–5410.

24 D. S. Brauer, N. Karpukhina, M. D. O'Donnell, R. V. Law and R. G. Hill, *Acta Biomater.*, 2010, **6**, 3275–3282.

25 R. A. Martin, H. Twyman, D. Qiu, J. C. Knowles and R. J. Newport, *J. Mater. Sci.: Mater. Med.*, 2009, **20**, 883–888.

26 E. Gentleman, Y. C. Fredholm, G. Jell, N. Lotfibakhshaiesh, M. D. O'Donnell, R. G. Hill and M. M. Stevens, *Biomaterials*, 2010, **31**, 3244–3252.

27 E. Gentleman, M. M. Stevens, R. G. Hill and D. S. Brauer, *Acta Biomater.*, 2013, **9**, 5771–5779.

28 L. L. Hench and H. A. Paschall, *J. Biomed. Mater. Res.*, 1973, **7**, 25–42.

29 J. R. van Wazer and K. A. Holst, *J. Am. Chem. Soc.*, 1950, **72**, 639–644.

30 J. R. van Wazer, *Phosphorus and its compounds*, Interscience, New York, 1958.

31 K. J. D. MacKenzie and M. E. Smith, *Multinuclear solid-state NMR of inorganic materials*, Elsevier Science, Amsterdam, Pergamon, 2002.

32 C. Roiland, F. Fayon, P. Simon and D. Massiot, *J. Non-Cryst. Solids*, 2011, **357**, 1636–1646.

33 R. E. Youngman, U. Werner-Zwanziger and J. W. Zwanziger, *Z. Naturforsch. A Phys. Sci.*, 1996, **51**, 321–329.

34 F. Fayon, G. Le Saout, L. Emsley and D. Massiot, *Chem. Commun.*, 2002, **16**, 1702–1703.

35 S. L. Friess, *J. Am. Chem. Soc.*, 1952, **74**, 4027–4029.

36 D. S. Brauer, in *Bio-glasses - an introduction*, ed. J. R. Jones and A. G. Clare, Wiley, New York, Chichester, Brisbane, Singapore, Toronto, 2012, ch. 4, pp. 45–63.

37 J. F. McCullough, J. R. van Wazer and E. J. Griffith, *J. Am. Chem. Soc.*, 1956, **78**, 4528–4533.

38 I. Ahmed, M. P. Lewis, S. N. Nazhat and J. C. Knowles, *J. Biomater. Appl.*, 2005, **20**, 65–80.

39 B. C. Sales, L. A. Boatner and J. O. Ramey, *J. Non-Cryst. Solids*, 2000, **263**, 155–166.

40 J. C. Elliott, *Structure and chemistry of the apatites and other calcium orthophosphates*, Elsevier, Amsterdam, New York, London, Tokyo, 1st edn, 1994.

41 M. D. O'Donnell, S. J. Watts, R. G. Hill and R. V. Law, *J. Mater. Sci.: Mater. Med.*, 2009, **20**, 1611–1618.

42 N. Forler, F. Vasconcelos, S. Cristol, J. F. Paul, L. Montagne, T. Charpentier, F. Mauri and L. Delevoye, *Phys. Chem. Chem. Phys.*, 2010, **12**, 9054–9063.

43 T. M. Alam, B. C. Tischendorf and R. K. Brow, *Solid State Nucl. Magn. Reson.*, 2005, **27**, 99–111.

1134 | *J. Mater. Chem. B*, 2015, **3**, 1125–1134

This journal is © The Royal Society of Chemistry 2015